

SUPPORTING INFORMATION

Tethering of the IgG1 Antibody to Amorphous Silica for Immunosensors development: A Molecular Dynamics Study

Didac Martí,^{1,2} Jon Ainsley,^{1,3} Oscar Ahumada,⁴ Carlos Alemán,^{1,2,5} Juan Torras^{1,2,*}*

¹ Department of Chemical Engineering (EEBE). Universitat Politècnica de Catalunya, C/Eduard

Maristany 10-14, Ed I2, 08019, Barcelona, Spain

² Barcelona Research Center for Multiscale Science and Engineering, Universitat Politècnica de

Catalunya, C/Eduard Maristany 10-14, 08019, Barcelona, Spain

³ Cancer Therapeutics Unit, The Institute of Cancer Research, 15 Cotswold Road, Sutton,

London SM2 5NG UK

⁴ Mecwins S.A., Ronda de Poniente 15, Tres Cantos, Madrid, 28760, Spain

⁵ Institute for Bioengineering of Catalonia (IBEC), The Barcelona Institute of Science and

Technology, Baldiri Reixac 10-12, 08028 Barcelona, Spain

Page	Content
S2-S4	Methods and results describing the simulations on silicate surface structure.
S5	Table S1. Density and geometric parameters of amorphous silica.
S6	Table S2. Radius of gyration for the free and immobilized IgG1 protein.
S7	Table S3. Geometric parameters used to define the orientation of immobilized IgG1 with respect to the surface.
S8.	Figure S1. Structure of cristobalite used as starting point to generate the amorphous SiO ₂ model. Obtained SiO ₂ glass model. Radial distribution functions (RDFs) of amorphous silica.
S9	Figure S2. Temporal evolution of the root mean square displacement (RMSD) of the C ^α atoms of IgG1 immobilized on amorphous silica.

Methods

Silica surface model

A slab of amorphous silica was built to simulate the outermost layer of amorphous silica located on the top of the sensor surface. This was performed by applying the procedure reported by Huff *et al.*^{S1} to convert α -cristobalite into amorphous silica. More specifically, a α -cristobalite slab of $50 \times 50 \times 20 \text{ \AA}^3$ was constructed and, subsequently, subjected to a rigorous annealing process by applying several heating and quick cooling processes. The annealing process was conducted using a MD approach as implemented in the DLPOLY 4 program^{S2} and applying the Tersoff potential for bulk silica.^{S3} After applying the Huff *et al.*'s protocol, an additional set of less extreme but longer annealing cycles was performed until an amorphous tetrahedral silica structures without defects was obtained. Tetrahedral silica structures were identified by means of radial distribution functions and its integration to obtain the coordination numbers. The annealing process entailed three cycles of heating at 1500 K (for 0.5 ns), which was followed by cooling at 1000K, 500K and 298 K for 0.2 ns each, followed by a 4.5 ns of NPT MD ensemble at 298 K and 1 bar. After the final annealing process, the slab was replicated 10 times in the x - and y -axis in order to obtain a larger slab of $500 \times 500 \times 20 \text{ \AA}^3$ (to avoid interactions with periodic neighboring proteins) and relaxed using an NPT MD ensemble for 0.2 ns at 298 K. Finally, the large surface was hydrolyzed by randomly adding hydrogen atoms to the unsaturated surface oxygens, at the equilibrium distance, until a final density of 1.68 hydrogen atoms per nm^2 was reached.

RESULTS AND DISCUSSION

Silica surface structure

A slab of amorphous SiO₂ was modeled by MD using the cristobalite crystal structure as starting point MD and the Tersoff force field.^{S3} A SiO₂ glass model, which is compared in Figure S1a-b with the cristobalite crystal structure, was obtained after applying an annealing process, as described in the Methods section. The final density of the SiO₂ glass was 2.22 g/cm³, which perfectly matches the experimental value of 2.20 g/cm³.^{S4} On the other hand, Figure S1c shows the radial distribution functions (RDFs) of SiO₂ glass at 298 K. The distance of maximum probability obtained for the Si–O (1.61 Å), Si–Si (3.20 Å) and O–O (2.75 Å) bond contact (*i.e.* the most intense peak) are very close to experimental values,^{S4,S5} as is reflected in the comparison shown in Table S1. The existence of a small peak for the Si–Si and O–O radial distribution functions at a distance lower than 2.4 Å has been associated to some defects in the tetrahedral network that the annealing process could not fix. These defects represent ~2% of the whole bulk only and are not expected to interfere in the immobilization of the IgG1.

Calculated coordination numbers, which were obtained by integrating the area of the maximum probability peak of both Si–O and O–Si distribution functions, are of 4.0 and 2.0 for Si and O atoms, respectively, evidencing that the SiO₂ glass obtained presents an almost perfect tetrahedral network around the silicon atom. Table S1 lists the averaged O–Si–O and Si–O–Si bond angles. The averaged O–Si–O bond angle, 109.3°, is very close to the ideal tetrahedral geometry, which is fully consistent with the calculated coordination numbers obtained. Overall, the amorphous silica glass modeled in this work exhibits a structure similar to those obtained in previous calculations using other force fields.^{S6,S7}

The SiO₂ glass obtained was next used to model a large slab of amorphous silica by replicating along the *xy* plane. Before obtaining the final surface, a second annealing process was conducted to homogenize and dismiss possible defects due to the tessellation process. Finally, one of the

surface sides was hydroxylated by capping the unsaturated surface atoms of Si and O with –OH and –H, respectively. The hydroxylation process leads to a final density of 1.68 hydrogen atoms per nm².

REFERENCES

- S1. Huff, N. T.; Demiralp, E.; Çagin, T.; Goddard III, W. A. Factors Affecting Molecular Dynamics Simulated Vitreous Silica Structures. *J. Non-Cryst. Solids* **1999**, *253*, 133-142.
- S2. Todorov, I. T.; Smith, W.; Trachenko, K.; Dove, M. T. DL_POLY_3: New Dimensions in Molecular Dynamics Simulations via Massive Parallelism. *J. Mater. Chem.* **2006**, *16*, 1911-1918.
- S3. Munetoh, S.; Motooka, T.; Moriguchi, K.; Shintani, A. Interatomic Potential for Si–O Systems Using Tersoff Parameterization. *Comp. Mater. Sci.* **2007**, *39*, 334-339.
- S4. Mozzi, R. L.; Warren, B. E. The Structure of Vitreous Silica. *J. Appl. Crystallogr.* **1969**, *2*, 164-172.
- S5. Grimley, D. I.; Wright, A. C.; Sinclair, R. N. Neutron Scattering from Vitreous Silica IV. Time-of-Flight Diffraction. *J. Non-Cryst. Solids* **1990**, *119*, 49-64.
- S6. Takada, A.; Richet, P.; Catlow, C. R. A.; Price, G. D. Molecular Dynamics Simulations of Vitreous Silica Structures. *J. Non-Cryst. Solids* **2004**, *345-346*, 224-229.
- S7. Fogarty, J. C.; Aktulga, H. M.; Grama, A. Y.; van Duin, A. C. T.; Pandit, S. A. A Reactive Molecular Dynamics Simulation of the Silica-Water Interface. *J. Chem. Phys.* **2010**, *132*, 174704.

Table S1. Density (in g/cm³), bond distances (in Å) and bond angles (in °) of amorphous silica. Values correspond to the averages of the model derived in this work from MD simulations and to experimental measurements reported in the literature.

Amorphous SiO₂		This work	Experimental
Density		2.22	2.20 ^a
Bond distances	Si–Si	3.20	3.077 ^b , 3.12 ^a
	Si–O	1.61	1.608 ^b , 1.620 ^a
	O–O	2.75	2.626 ^b , 2.65 ^a
Bond angles	Si–O–Si	145.9	144 ^a , 153 ^c
	O–Si–O	109.3	109.5 ^a , 109.7 ^b

^a From: Mozzi, R.L., Warren, B.E., 1969. The structure of vitreous silica. *J. Appl. Crystallogr.* 2, 164-172.

^b From: Grimley, D.I., Wright, A.C., Sinclair, R.N., 1990. Neutron scattering from vitreous silica IV. Time-of-flight diffraction. *J. Non-Cryst. Solids* 119, 49-64.

^c From: Da Silva, J.R.G., Pinatti, D.G., Anderson, C.E., Rudee, M.L., 1975. A refinement of the structure of vitreous silica. *The Philosophical Magazine: A Journal of Theoretical Experimental and Applied Physics* 31, 713-717.

Table S2. Averaged radius of gyration (R_g , in Å) and its cartesian decomposition for the free and immobilized IgG1 protein. Data were obtained by analyzing the MD and REMD trajectories.

IgG1	Free	Immobilized	
T (K)	298	250	298
R_g	49.8	56.3	56.4
R_g^x	28.2	35.1	35.4
R_g^y	22.0	19.5	19.3
R_g^z	34.7	39.5	39.5

Table S3. Most populated values (in degrees) obtained for the geometric parameter described in Scheme 2. Data were derived from REMD trajectories at 250, 298 K (sorted by population in descendent order; the most populated in bold) and averaged over the whole range of temperatures (from 250 to 380 K).

Angle	250 K	298 K	Average ^a
α	24 ; 102 ; 90	66 ; 138 ; 36	82 \pm 26
β	70 ; 153 ; 128	102 ; 114 ; 81	99 \pm 18
γ	54 ; 72 ; 108	54 ; 114	54 \pm 10
φ	117 ; -87 ; -141 ; 45	-93 ; 109	-94 \pm 19 ; 116 \pm 5
θ	-12 ; 144 ; -162 ; -81	-3 ; 141 ; -132	-9 \pm 3

^a Average angle between all maximum probability angles obtained from the histogram at each REMD temperature.

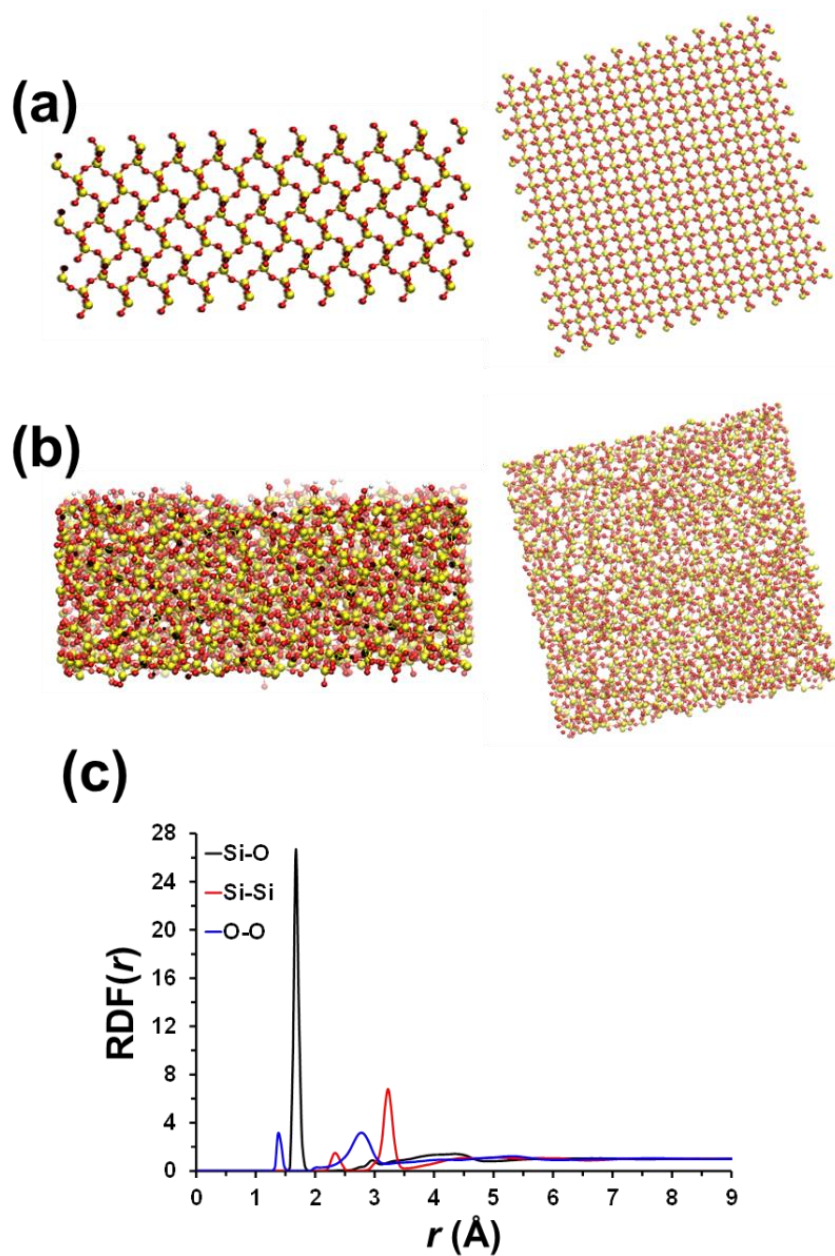


Figure S1. (a) Structure of cristobalite used as starting point to generate the amorphous SiO₂ model (axial and equatorial views in left and right, respectively). (b) Obtained SiO₂ glass model (axial and equatorial views in left and right, respectively). (c) Radial distribution functions (RDFs) of amorphous silica. RDFs of silica bulk for silicon-oxygen (Si–O), silicon-silicon (Si–Si) and oxygen-oxygen (O–O) distances are shown.

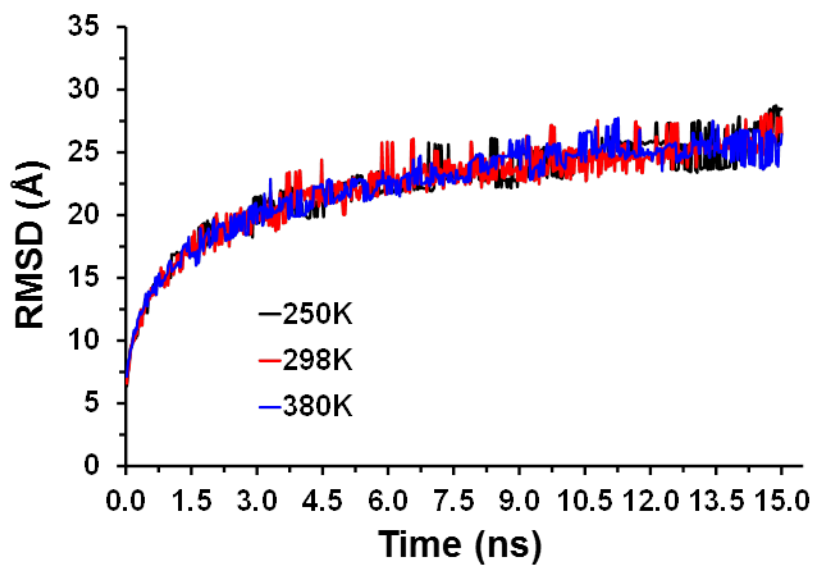


Figure S2. Temporal evolution of the root mean square displacement (RMSD) of the C^α atoms of IgG1 immobilized on amorphous silica during the 15 ns of REMD trajectories at 250, 298 and 380 K. As is shown, a stable behavior with low oscillations of the RMSD values was obtained beyond 4 ns in all cases, justifying the use of the last 11 ns of trajectory for the conformational analyses.